Journal of Radioanalytical and Nuclear Chemistry
https://doi.org/10.1007/s10967-020-07575-x

Decomposition of continuous soil–gas radon time series data observed at Dharamshala region of NW Himalayas, India for seismic studies

Sunil Dhar[1] · Surjeet Singh Randhawa[2] · Arvind Kumar[3] · Vivek Walia[3] · Ching-Chou Fu[4] · Harish Bharti[2] · Arun Kumar[1]

Received: 24 September 2020 / Accepted: 22 December 2020

Abstract
Soil–gas radon time series data has been generated at Dharamshala station for seismic studies in NW Himalayas, India. Compared with the influence of temperature and pressure, radon and rainfall have shown a strong correlation. Decomposition of radon time series into three component series (seasonal, trend, and residual) has been done for further recognizing the authentic anomalous values. The irregular patterns in daily and residual radon data have been associated with earthquake events and rainfall. This monitoring station found to be sensitive to the seismic events within a distance of about 70 km.

Keywords Time series analysis · Seismic event · Meteorological parameter · Earthquake precursor

Introduction

Earthquakes cause a remarkable menace to humankind. Over the past decade, it has been the dominating source of causality from universal calamity. By this, about 60,000 people in a year have lost their lives worldwide and about 90% of earthquakes occurred in developing countries [1]. Dharamshala region of Kangra valley of Himachal Pradesh, which is a part of NW Himalayas, is susceptible from a tectonic perspective. It is located in Zone IV of the seismic zoning map of India having many regional and local thrust faults [2]. The area has witnessed some major as well as minor earthquakes during the last century [2, 3]. Considerable harmful seismic events have battered the state and the adjacent parts of neighboring states (Punjab, Uttar Pradesh, and Jammu & Kashmir). A few of the noticeable seismic events that jolted the state are the Kangra earthquake 1905 of magnitude 8.0, the Kinnaur earthquake 1975 of magnitude 6.7, and the Dharamshala earthquake 1986 of magnitude 5.7. Apart from these symbolic earthquakes, more than 250 seismic events having a magnitude of 4 or more have also been recorded in the region, Inconsistent with other natural threats namely torrential rain, avalanche, etc. knock without any alarm and seriously influence humankind and their commercial losses. Until now in earth science, there is no comprehensive procedure to predict the time/location/magnitude of a coming earthquake.Possible geochemical precursors have been observed hours to months before some strong earthquakes at many sensitive and non-sensitive monitoring sites [4–8]. Sensitive sites are those sites that are more sensitive by a relatively small seismic shaking or stress increase. They are usually found along with or around active faults [9, 10] and considered as a potential location for earthquake precursory research. Among the geochemical precursors, radon (^{222}Rn) is proved to be one of the most promising geochemical precursors [11–19]. It has been also observed from the monitoring of ^{222}Rn in soil and groundwater that spatial and temporal variations can give valuable clues about geodynamical events. Additionally, ^{222}Rn has proven to be very useful as a tracer to understand greenhouse gases behaviors

✉ Arvind Kumar
kumararvind79@hotmail.com

✉ Vivek Walia
vivekwalia68@gmail.com

1 Department of Environmental Sciences, Central University of Jammu, Jammu and Kashmir, UT, India

2 State Centre for Climate Change, HP Council for Science Technology and Environment (HIMCOSTE), Shimla, Himachal Pradesh, India

3 National Centre for Research on Earthquake Engineering, National Applied Research Laboratories, Taipei, Taiwan

4 Institute of Earth Sciences, Academia Sinica, Taipei, Taiwan

Published online: 20 January 2021

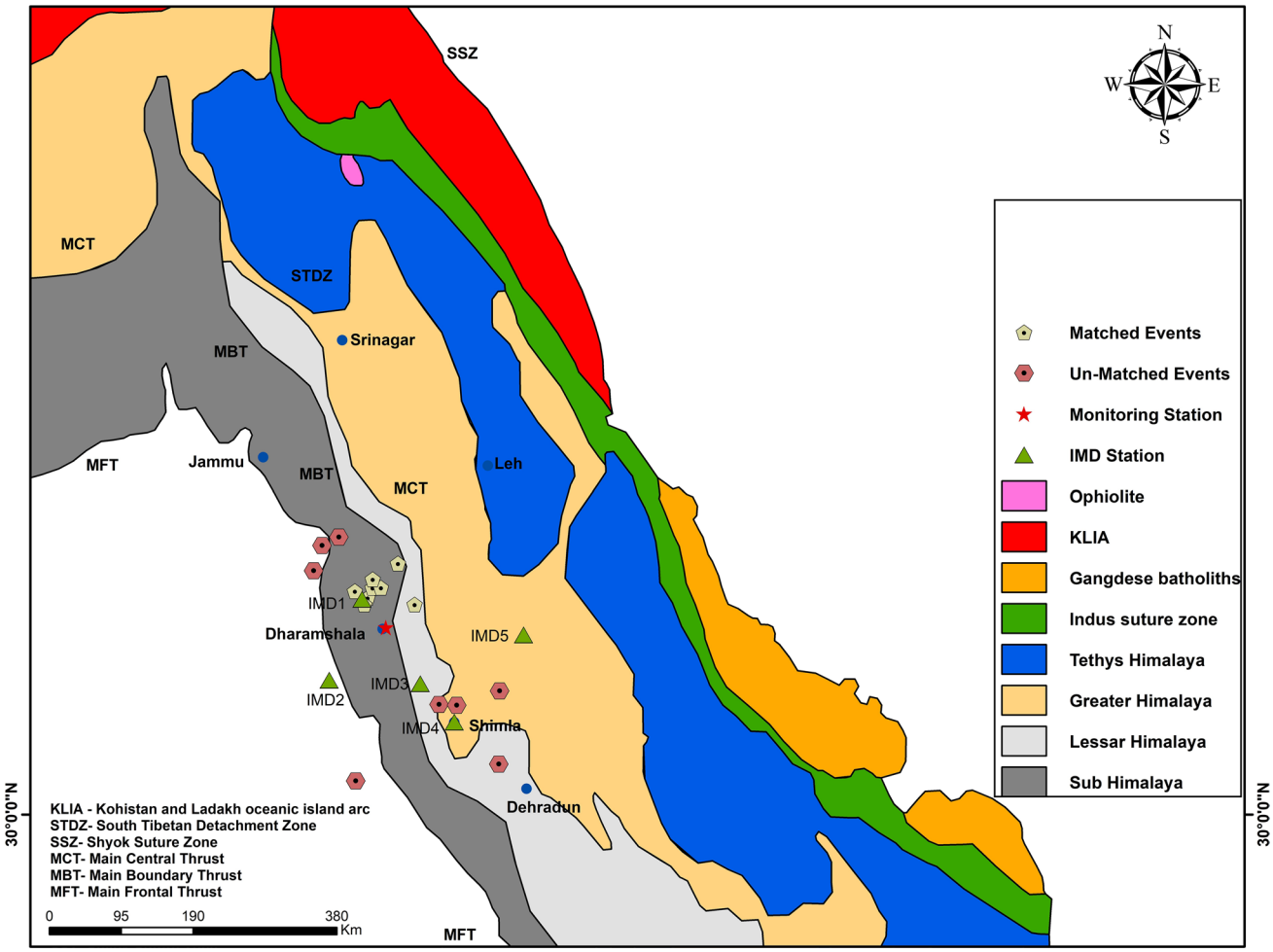

Fig. 1 The geological map showing the location of radon monitoring station and location of India Meteorological Department (IMD) monitoring stations in Himachal Himalayas, India (IMD-1 Dalhousie, IMD-2 Pong, IMD-3 Sunder Nagar, IMD-4 Shimla, and IMD-5 Kalpa). It is also showing all of the earthquake events which satisfied or not satisfied our selection criteria recorded in our study time

in the atmosphere, and their interchange with the soil [20]. A relatively high amount of ^{222}Rn data has been monitored in many countries both by grab and steady modes [21]. Several components that affect radon emanation coefficient and exhalation in soil have been reported [22–24]. There exists a strong correlation between the porosity and the radon emanation and the porosity and the exhalation [25]. Emanation controls the movement of radon atoms from within solid grains into free spaces of materials (pores, micropores, cracks). Whereas the exhalation rate is a measure of the liberation of radon from inside a sample to outside the sample [26]. The anomalous changes in the concentration of radon provide evidence in seismo-tectonic disturbances [27–29]. However, soil–gas radon emanation and exhalation from the bottom of the earth towards the surface is also affected by environmental parameters such as rainfall, temperature relative humidity, and pressure [30–35]. The shared daily cycles, local multi-hours, and multi-day radon signals, and shared periodic annual and semi-annual radon signals have been reported by Siino et al. [36] in their radon monitoring network in Italy. According to them, variations of atmospheric pressure and temperature would be responsible for short-term periods while for long-term ones seasonal rainfall cycles are likely to play an important role. As the radon emanation is not only affected by seismic events but also by meteorological parameters. Therefore, it is often not possible to identify radon anomalies or radon irregular patterns caused by seismic events, and those merely caused by climate changes. Some anomalies are hidden whereas some anomalies are erroneously considered as earthquake precursors.These necessities the usage of statistical and computational tools to minimize the effects of meteorological parameters on radon emission [32, 33, 37, 38]. In the present study, the correlation between observed radon using a barasol probe in the Dharamshala region of Kangra Valley in NW Himalayas (Fig. 1) and metrological parameters

have been calculated using a Pearson correlation. Also, seasonal changes and trends in continuous soil–gas radon time series have been removed for obtaining residual radon using the time series decomposition method. With the aim to recognize authentic radon anomalous values or irregular patterns, observed radon time series together with residual radon has been correlated with seismic events and metrological parameters.

Geology of the study area

Geologically the study area consists of rocks of the Siwalik Group (Outer Himalaya) and the Lesser Himalayan zone [39]. Rock types of the Siwalik Group are dominantly represented by sedimentary sequences of mudstone, shale, clay, coarsely bedded the conglomerate and sandstones of Middle Miocene to Upper Pleistocene times. The lesser Himalayan zone, comprising lower tertiary Dharamshala sandstones and Sabathu shales, early Precambrian slates, phyllites, schists limestones and basic lava flows followed by late Precambrian Dhauladhar granites and gneisses dominate the study area. Lesser Himalayan zone rocks are over thrust over the Siwalik formation along with a series of major thrust planes, the Main Central thrust (MCT), the Main Boundary Thrust (MBT), and the Himalayan frontal thrust (HFT) which came into existence during the collision of the Indian and Eurasian converging plates [40, 41]. Further, the region is traversed by numerous faults and lineaments that cross-cut the litho-units of the region transversely controlling the main structural pattern and high seismicity [40] and related geological attributes viz. development of a significant amount of secondary structurally controlled porosity and permeability along fractured joints, fault zones and formation contacts [42, 43].

Experimental

In the present study, the Barasol radon probe (BMC2[1]) produced by Algade France has been utilized for a steady recording of radon, temperature, and pressure in soil gas. It is formed of a sensor (Silicon alpha sensitive detector) that notes the radon gas go into the detection chamber. The BMC2 probe consists of an observation unit, electronics, and a cell unit shaped inside an instrument consisting of a tube made of an epoxy glass material 61 mm in diameter and 500 mm long [44]. As a norm, an eight-pin connector brings the probe interconnection and control. The connector has an air and watertight index of IP 68 when covered by the cap. The battery unit has space for two batteries of 1.5 V. We have used alkaline batteries because of their longer shelf life than other batteries. Two alkaline batteries provide the probe for more than 6 months of self-supporting action. It can store data for 1 year.

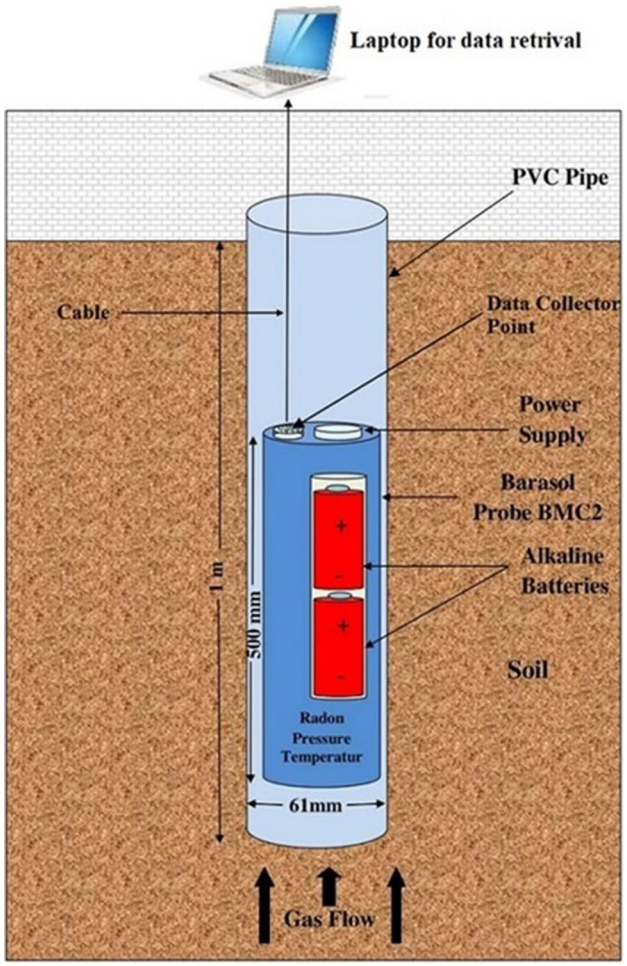

Fig. 2 The sketch showing the observational method used in the present study. The structure of the observation hole, BMC2 position, data collector, and power supply

BMC2 as well as all-solid-state radon detectors are characterized by a strong performance dependence from absolute humidity [45]. The response of radon monitors employing semiconductor detectors needs to be corrected as a function of absolute humidity. Especially if an electrostatic collection of the short-lived radon daughters take place and/or big sized detection volumes are adopted. Water molecules cause the neutralization of radon progenies, reducing the detector efficiency [45, 46].

It is installed in the hole at a depth of 1.0 m by casing this hole with the PVC pipe with 15 min radon monitoring time interval at the Dharamshala station of Kangra Valley in NW Himalayas, India (Fig. 2). The outside of the PVC pipe was covered with the steel casing to protect the monitoring station from extreme weather conditions.

[1] Barasol Multi Capteurs.

Methods

Pearson correlation coefficient

Pearson's correlation coefficient (r) is defined as a measure of the strength of the relationship between two variables and their correlation [47]. In a few words, r estimated the effect of one variable when another variable changes. The correlation coefficient formula can find the relationship between variables. It returns the values between − 1 and 1. Following is the Pearson coefficient correlation formula to measure the strength of two variables.

$$r = \frac{NSXY - SXSY}{\sqrt{\left[NSX^2 - (SX)^2\right]\left[NSY^2 - (SY)^2\right]}} \quad (1)$$

where N is the number of pairs of data points, ΣXY is the sum of the products of paired data points, ΣX is the sum of X data points, ΣY is the sum of Y data points, ΣX^2 is the sum of squared X data points, and ΣY^2 is the sum of squared Y data points.

Time series decomposition

Time series data can display various patterns. It has always valuable to break the time series into several components, each of which represents a hidden pattern category.

The three forms of time series patterns: trend, seasonality, and cycles. During the process of decomposing a time series into its components, the trend and period are normally joined into a single trend-cycle component (occasionally it is called a trend for clarity). Therefore, it is believed that time series consists of three components: a trend-cycle component, a seasonal component, and a remainder component (containing anything else in the time series). If an additive decomposition is assumed, then it can be written as

$$Y_t = S_t + T_t + R_t \quad (2)$$

where Y_t = the data, S_t = the seasonal component, T_t = the trend-cycle component, and R_t = the remainder component, entire at period t. In lieu of, a multiplicative decomposition would be written as

$$Y_t = S_t \times T_t \times R_t \quad (3)$$

If the magnitude of seasonal fluctuations or changes around the trend cycle does not change with the level of the time series, additive decomposition is applicable. And when changes in seasonal patterns or changes around the trend cycle seem to be comparative to the level of the time series, multiplicative decomposition is applicable. Multiplicative decompositions are common with economic time series. An alternative to employing a multiplicative decomposition is to first convert the data down to the fluctuation in the series come out to be steady over time, then apply an additive decomposition. When a log transformation has been used, this is equivalent to using a multiplicative decomposition because

$Y_t = S_t \times T_t \times R_t$ is equivalent to $Log\, Y_t = Log\, S_t + Log\, T_t + Log\, R_t$

Results and discussion

In the present study, the characteristics of temporal variability of soil–gas radon concentrations at the Dharamshala monitoring station has been examined. To make the continuity and regularity of the data, the data has been carefully selected for intervals with minimum breaks. The breaks in the data may be due to power loss, as sometimes batteries drain out before the battery replacement dates. We cannot see that the sensor at the station is working or not as this monitoring, is not real-time. The selected soil–gas radon concentrations data along with temperature, pressure, and rainfall of years 2016 and 2017 are shown in Fig. 3a and b. We recorded anomalously high radon value at some points in the year 2016. Those anomalously unexpected high radon values may be due to the malfunctioning of equipment or due to meteorological electric and electromagnetic activity [33, 45] or other unknown reasons. Radon instruments can be to be vulnerable to close exposure of the small electric spark and they produced spurious counts. These values may cause unnecessary high deviation and have perturbed the real anomalies [48–50]. These values have been replaced with the average of neighboring values. It is the general criteria being used at the International level [44, 48–51] for defining radon anomalies with better accuracy. Figure 4a and b show the soil–gas radon concentrations data after neglecting anomalously high radon values along with temperature, pressure, and rainfall of years 2016 and 2017. The rainfall data from the India Meteorological Department (IMD), the government of India has been obtained from the nearest weather station i.e. IMD-1 Dalhousie (Fig. 1). Rainfall data was available with daily sampling, so for the sake of uniformity and comparison 15-min radon, temperature, and pressure data have been reduced to daily averages (Fig. 4a, b).

To find a radon correlation with temperature, pressure, and rainfall, we have used Pearson correlation. It computes in what way two continual signals co-vary overtime and point out the linear relation as a number within − 1 (negative correlation) to 0 (no correlation) to 1 (perfectly correlated). In a negative correlation, one variable increases as the other decreases, and vice versa. The computed overall Pearson (r)

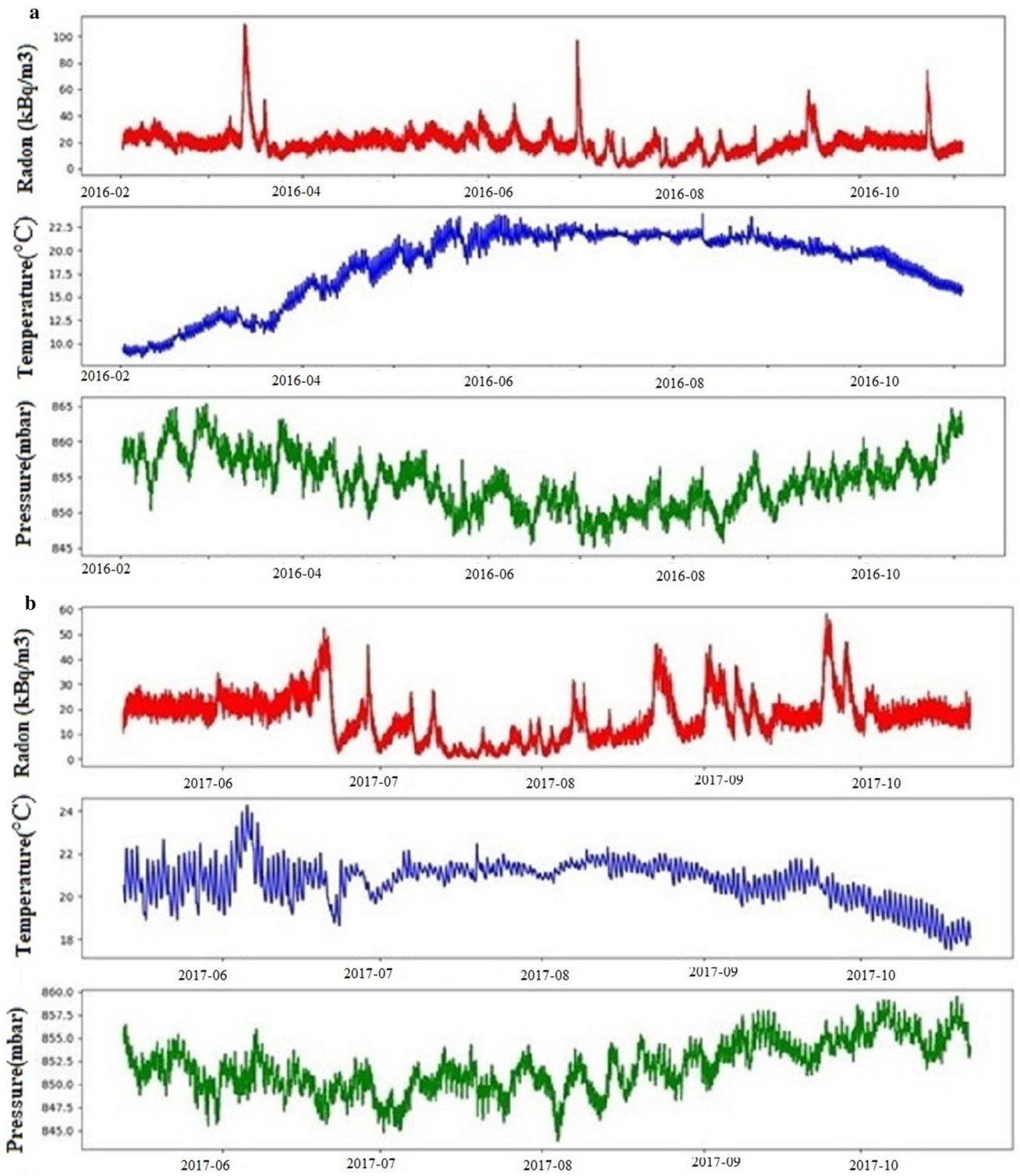

Fig. 3 Recorded soil-gas radon concentrations along with temperature, pressure, and rainfall at the Dharamshala monitoring station, NW Himalaya, India. **a** for the year 2016 and **b** for the year 2017

between radon and temperature for 2016 and 2017 in our study is weak and negative i.e. − 0.28 and − 0.23, respectively (Fig. 5a, b). When temperature changes, a temperature gradient appears between the bottom and the top of the hole where radon concentrations are measured. This leads to changes in pressure gradient and of concentration [52,

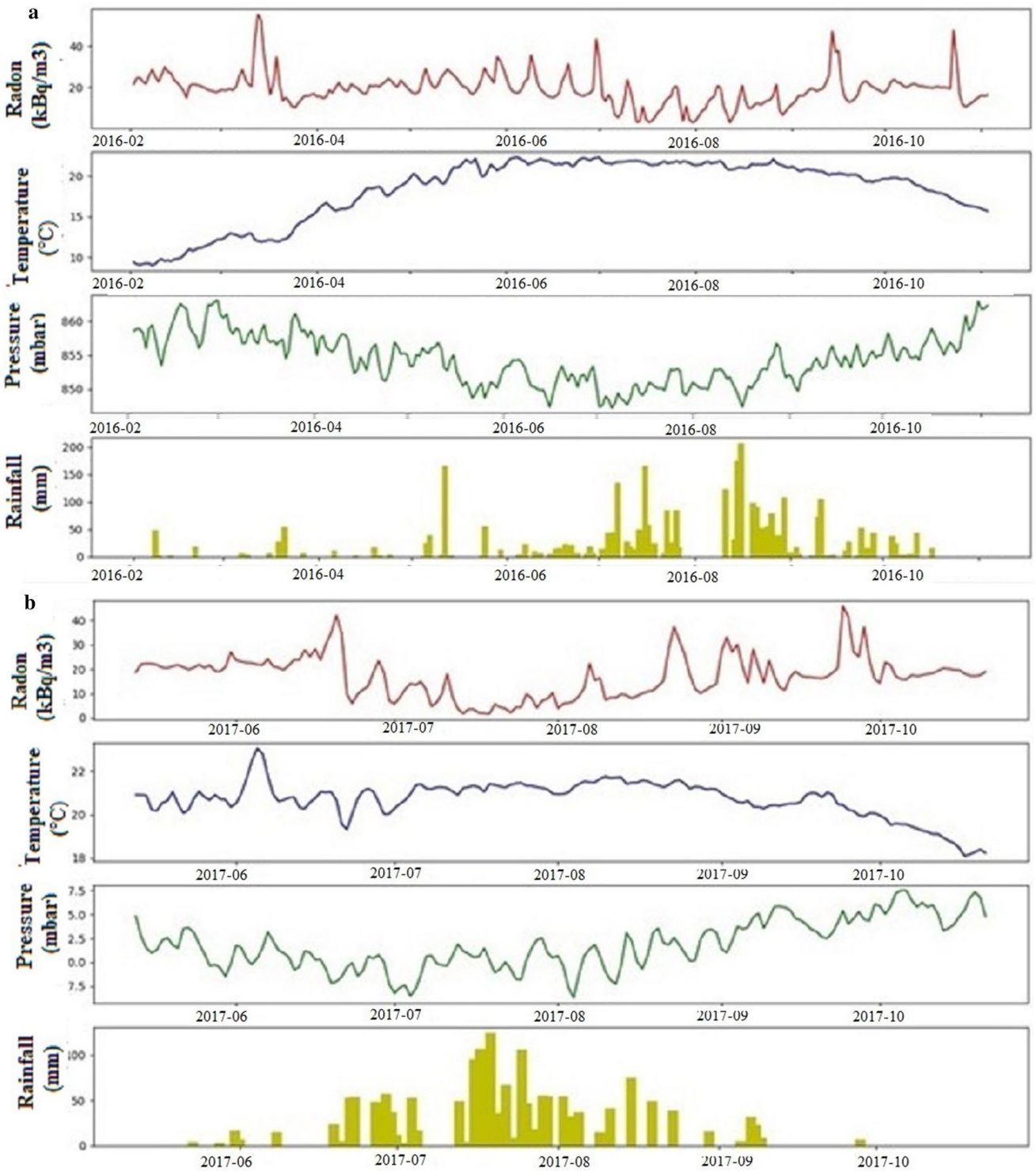

Fig. 4 Daily soil-gas radon concentrations along with temperature, pressure, and rainfall at the Dharamshala monitoring station, NW Himalaya, India. **a** for the year 2016 and **b** for the year 2017

53] Fig. 6 a and b shows the computed overall Pearson (r) between radon and pressure for 2016 and 2017 are 0.22 and 0.26, respectively. The role of atmospheric pressure on radon transport is well known for its pumping or piston effect [54, 55]. Various studies in different countries have reported no correlation [56] negative correlation [32, 57], and positive correlation [56–58] of radon with temperature and pressure. Siino et al. [36] have reported a different correlation of radon

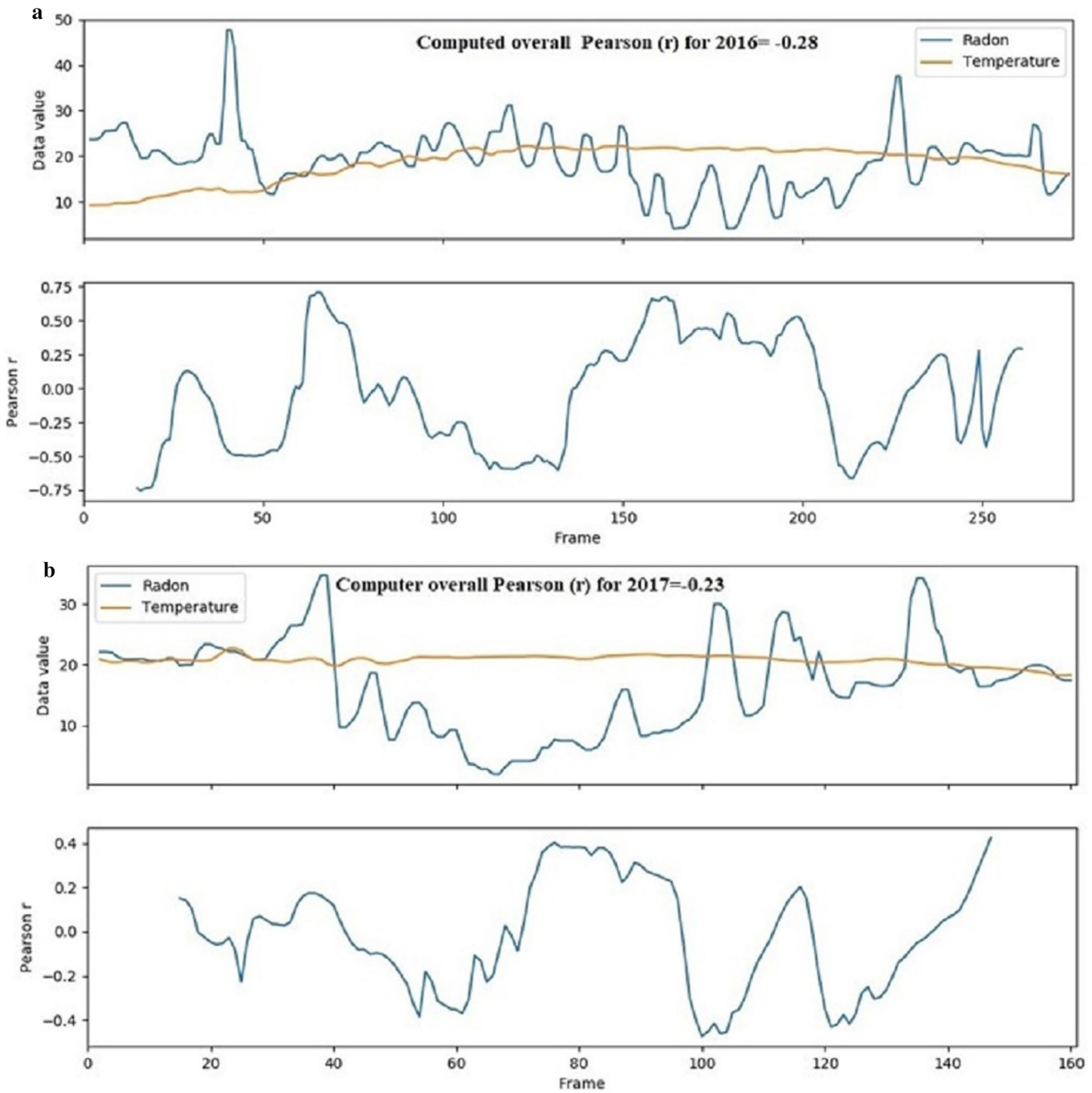

Fig. 5 The computed overall Pearson (*r*) between radon and temperature and moment-to-moment, local synchrony between radon and temperature using Pearson correlation, repeated along with a rolling window of 30 days **a** for year the 2016 and **b** for the year 2017 at the Dharamshala monitoring station, NW Himalaya, India

with temperature and pressure for their nine monitoring stations in Italy. It is noticed that there is not a uniform and stable relations between radon and meteorological variables but that this relationship is complex and site-dependent.

The computed overall Pearson (*r*) between radon and rainfall for 2016 and 2017 are −0.15 and −0.38 respectively (Fig. 7a, b). The radon emanation rates are extremely reduced by heavy rainfall because the water fills the empty pores and reduces the diffusion of radon [33]. After rainfall, the exhalations are rapidly recovered and increased [56].

The Total Pearson (*r*) is an estimate of overall synchrony that weakens the interconnection between two signals to an individual value. Despite that, there is an approach to see from moment-to-moment, local synchrony, using Pearson correlation. One method to do this is by calculating the Pearson correlation in a short section of the signal, and redo

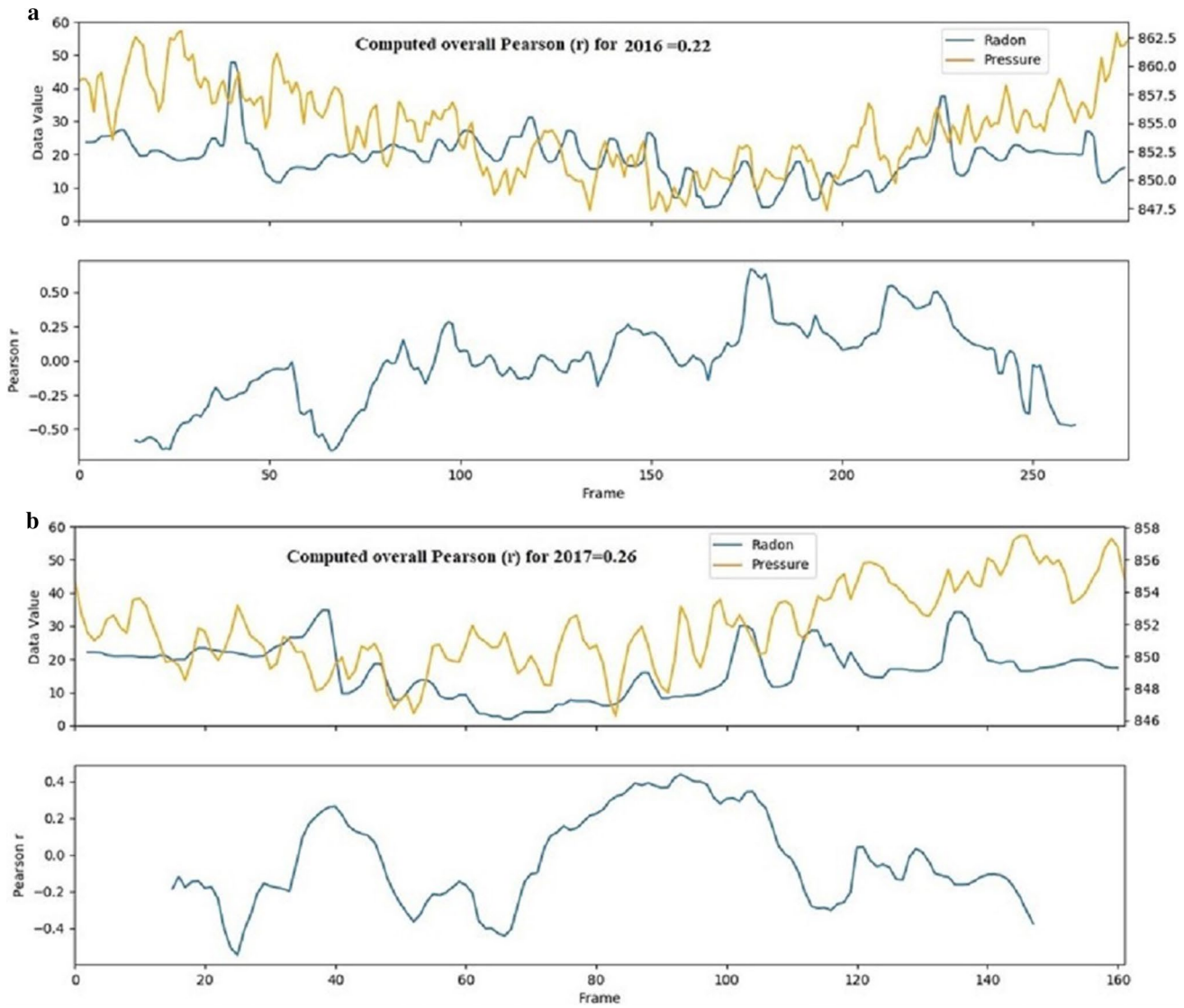

Fig. 6 The computed overall Pearson (r) between radon and pressure and moment-to-moment, local synchrony between radon and pressure using Pearson correlation, repeated along with a rolling window of 30 days **a** for the year 2016 and **b** for the year 2017 at the Dharamshala monitoring station, NW Himalaya, India

the action forward with a rolling window as far as the total signal is completed. In our study, we have calculated the Pearson correlation in the radon signal, and redo the action forward with a rolling window of 30 days until all signal is completed (Figs. 5, 6 and 7). It is clear from these figures that radon is not only restraint by single metrological parameters but multi metrological parameters. Apart from meteorological parameter fluctuations, there are possibly more variables that influence the radon emission such as soil permeability and soil porosity [59, 60] and such dependence can be sophisticated differing from location to location and leading consequently to location-specific characteristics of the radon [58, 61]. There is a need for having more than one variable investigation using detailed statistics means for better recognition of the characteristics of radon emission [36].

Compared with the influence of other meteorological parameters, we found that there is a strong correlation between the exhalation rate with the precipitation (Figs. 5, 6 and 7). Also, from moment-to-moment, local synchrony between radon and rainfall (Fig. 7) that if the rainfall is heavy and cumulative, the radon values are low. This decay of radon after the downturn of precipitation is exponential; one possible reason is the natural decay of radon with a half-life of 3.84 days, and the second reason is the weakening of the capping effect [33]. Piersanti et al. [60] from his continuous radon monitoring in Italy has also observed that after a major precipitation episode radon

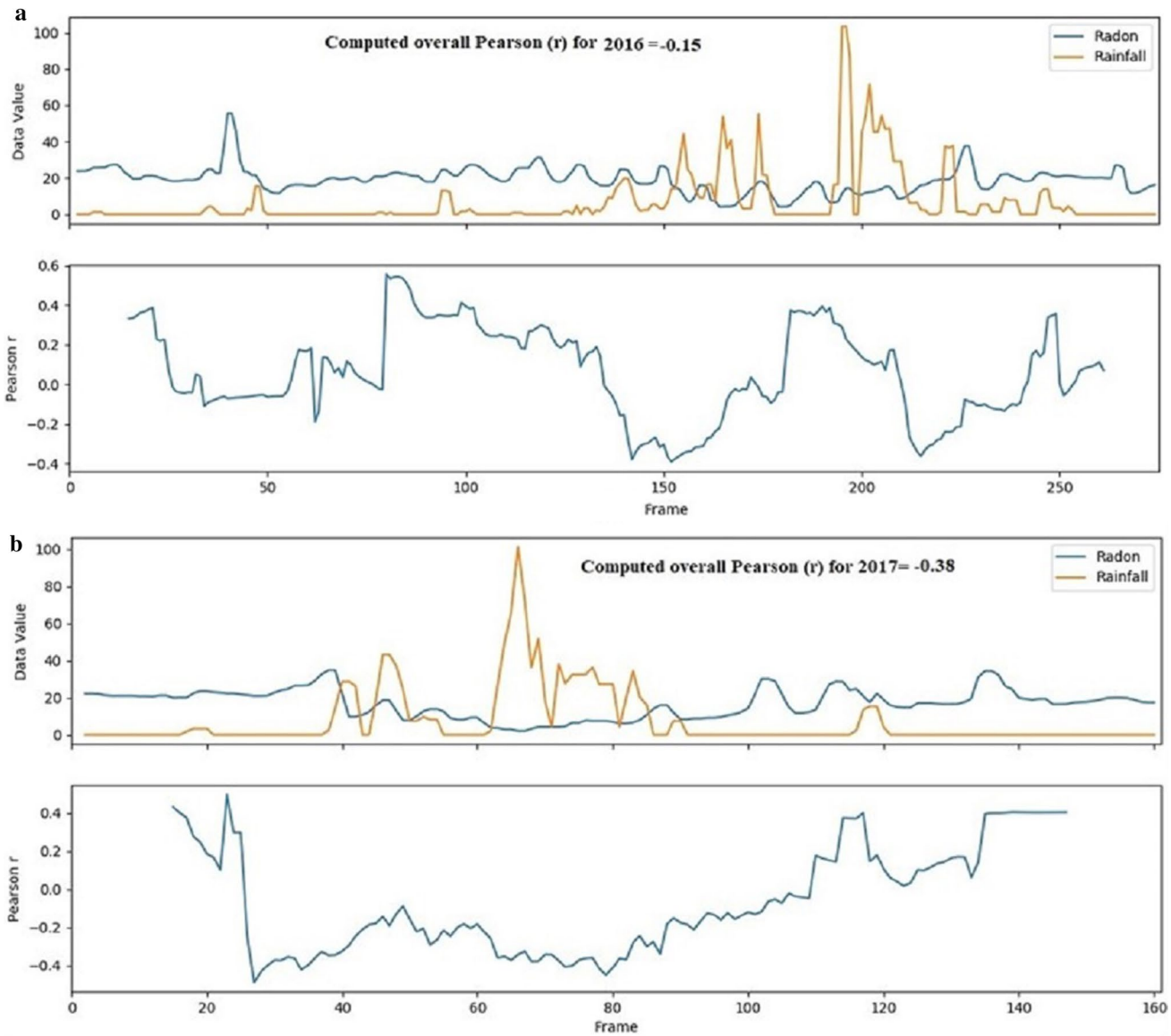

Fig. 7 The computed overall Pearson (*r*) between radon and rainfall and moment-to-moment, local synchrony between radon and pressure using Pearson correlation, repeated along with a rolling window of 30 days **a** for the year 2016 and **b** for the year 2017 at the Dharamshala monitoring station, NW Himalaya, India

concentration drastically falls by a factor greater than 10 up to a factor of almost 100. Arora et al. [33] from their study in Taiwan has found a strong effect of rainfall on radon. They found at the beginning of rainfall, radon showed a step transition and reached a peak with a time lag of 12–15 h. They have also found that radon after attaining a peak immediately after the rainfall shows regular recession in a complex manner after the long sequences of rainfall. Kulali et al. [56] from their study in Turkey has observed a significant correlation in the relation to the exhalation rate with the precipitation. The exhalation rates are extremely reduced by heavy rainfall. The impact of temperature and pressure on radon is not as substantial as the effect of rainfall in this study.

Figure 4a and b indicates a few periods of abnormal rise and fall of radon for 2016 and 2017 around the cumulative rainfall or may be due to some seismic events in the study areas. When an earthquake happens, faults in the bedrock boost radon emanation. Radon gas is drifted up to the soil surface by the inner fluids. Then the amount of radon meeting the surface of the soil is larger than the usually recorded values [13, 62].

This preliminary investigation of irregular patterns in radon concentrations at some points has been subjected to a detailed analysis to authenticate the results. This detailed analysis includes the decomposition of time series. Time series decomposition is the mathematical process of

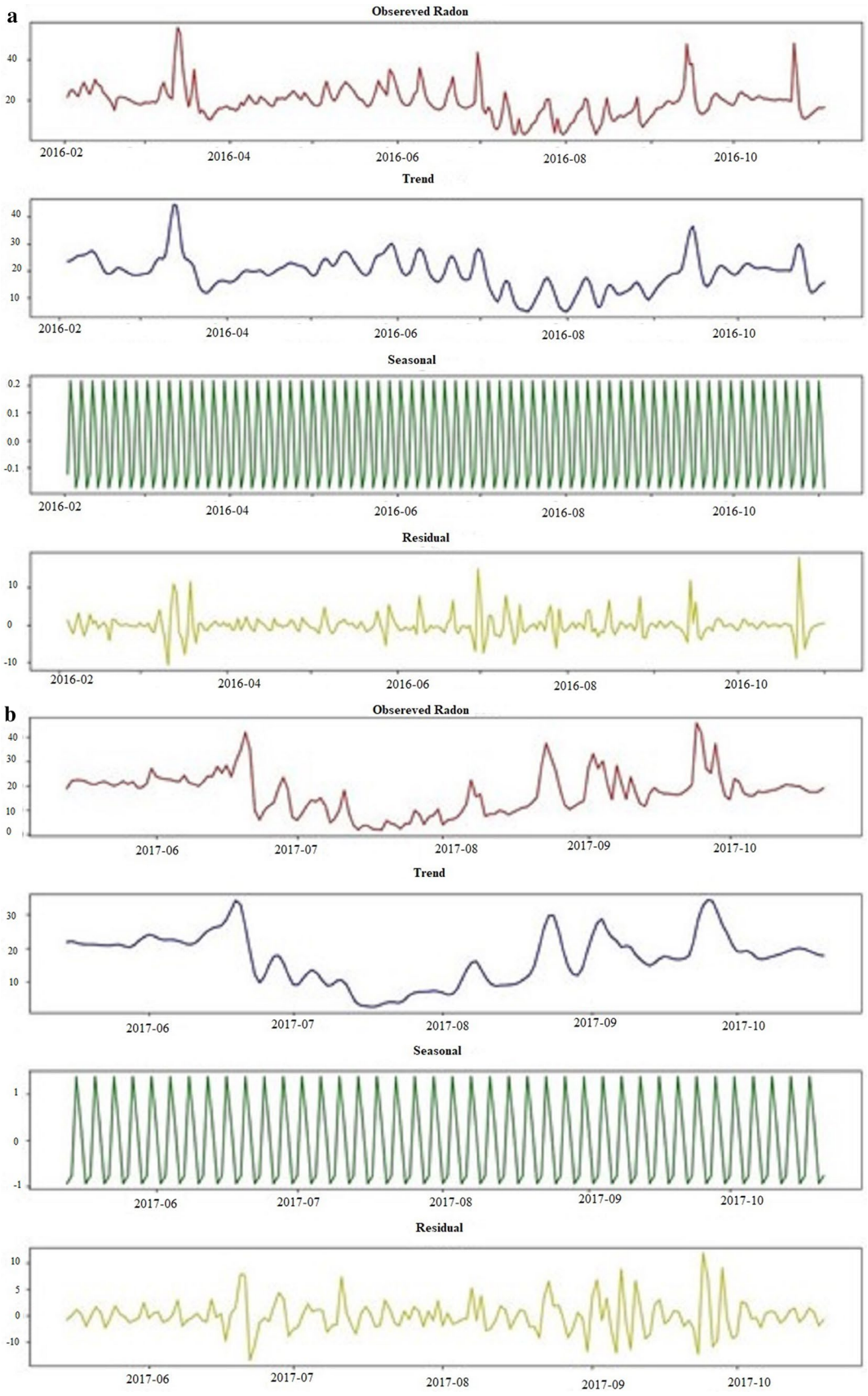
a
Obsereved Radon
40
20
2016-02
2016-04
2016-06
2016-08
2016-10
Trend
40
30
20
10
2016-02
2016-04
2016-06
2016-08
2016-10
Seasonal
0.2
0.1
0.0
-0.1
2016-02
2016-04
2016-06
2016-08
2016-10
Residual
10
0
-10
2016-02
2016-04
2016-06
2016-08
2016-10
b
Obsereved Radon
40
30
20
10
0
2017-06
2017-07
2017-08
2017-09
2017-10
Trend
30
20
10
2017-06
2017-07
2017-08
2017-09
2017-10
Seasonal
1
0
-1
2017-06
2017-07
2017-08
2017-09
2017-10
Residual
10
5
0
-10
2017-06
2017-07
2017-08
2017-09
2017-10

◂**Fig. 8** Decomposition of radon time series (from the top first panel is observed radon, the second panel is a trend, the third panel is seasonal, and the fourth panel is residual) using Statsmodels **(a)** for the year 2016 and (b) for the year 2017

converting a time series into multiple different time series. The original time series is often split into three component series (seasonal, trend and random). When a series shows periodic fluctuations based on the season (for example, every month/quarter/year), there is a seasonal component.

Seasonality is often of a set and known period. The trend component is the long-term increase or decrease of the information, which cannot be linear. Sometimes it would change direction as time increases. Random is additionally called noise, irregular or remainder; this can be the residual time series from the initial ones after removing the seasonal and trend variations. There are several ways to decompose a time series [63, 64]. The classic decomposition method commenced within the 1920s and maybe a comparably simple process. Classical decomposition has two forms, additive decomposition, and multiplicative decomposition. Within the additive decomposition, the overall data is taken as the sum of the decomposed patterns. Whereas during a multiplicative decomposition, the given time series data are treated as the product of the decomposed patterns [65].

In the present study, we have used Panda's library for the radon time series decomposition, which offers a lot of flexibility when manipulating data, and allowing us to perform statistical computing in Python. Statsmodels provides a convenient seasonal decomposition function, which can perform seasonal decomposition immediately. It can be ready with inborn datasets so we can put a time-series dataset directly into memory. Figure 8a and b show the decomposition of the radon time series (observed radon, trend, seasonal, and residual) using Statsmodels for 2016 and 2017. There are some clear trends but the seasonal composition of radon doesn't exist. The third curve in the figure shows the regular periodic fluctuation of about four days. This may correspond to the natural decay of radon with a half-life of 3.84 days.

Besides this, radon time series decomposition has been done by a polynomial fitting method to authenticate our results further. It is a well-known method that utilizes the classical statistical technique of regression analysis to estimate the parameters of low order polynomials, such as the linear and quadratic [66]. Here we have defined an order of polynomial three to fit in our data and find out the coefficient. Firstly, we found the overall trend in the radon time series, and then we have reduced the overall trend component from the original radon time series. After that, we found a seasonal component, and then we have reduced this seasonal component from the original radon time series. Finally, the overall trend and seasonal component have been reduced from the original radon time series to reach the residual component. Figure 9a and b show the decomposition of radon time series (observed radon, de-trend, deseasonal, and residual) using a polynomial fitting method for 2016 and 2017. There are also irregular patterns in residual radon data of 2016 and 2017.

To correlate the residual radon data with the earthquake that occurred in the study area during the observation time, only earthquakes with a magnitude two or more, depth ≤ 40 km, epicentral distance $(R) < 100$ km, and D/R ratio ≥ 1 (where $D = 10^{0.43M}$ theoretical strain radii of impending earthquakes proposed by Dobrovolsky [67] has been selected. Also, in the case of a group of the earthquake that is close together reported during our study time, we have selected the largest earthquake before the anomaly [44, 68]. The seismic data has been taken from IMD, Government of India. Figure 1 shows the location of IMD monitoring stations in Himachal Himalayas and a number of seismic events that matched or not matched our criteria reported during our study time. Numerous statistical methods have been used by different authors in the past to identify probable threshold values of the anomalous radon concentration or irregular patterns of radon [6, 48, 68, 69]. The most trusted method is considering the average (Avg.) + 'n' standard deviation (σ) as an anomaly in soil–gas and is found to be appropriate for soil–gas survey interpretations [48, 50, and 69]. In our study, radon concentration the statistical threshold value of gas anomalies or irregular patterns is fixed at the Avg. + 2σ. Figure 10a and b shows the daily radon, residuals radon calculated from Statsmodel and polynomial fitting method along with seismic events and rainfall that occurred during the study time. In 2016, four earthquake events that satisfy our criteria having different magnitudes (3.4, 2.8, 4.2, and 3.7) which occurred on March 30, 2016, May 22, 2016, August 28, 2016, and November 16, 2016, respectively have been reported by IMD (Table 1). The irregular patterns in daily radon, as well as residual radon data calculated from Statsmodel and polynomial fitting method, have been observed before the first and fourth earthquake events (purple rectangles in Fig. 10a). Before the third earthquake event, irregular patterns in residual radon data calculated by Statsmodel has been observed, whereas, residual radon value calculated by polynomial fitting method observed to be close to average (Avg.) plus two standard deviations (2σ). However, no irregular patterns have been found in normal daily radon variations. This may be due to the combined effects of the rainfall as well as earthquakes during this time. No irregular patterns in daily and residual radon data have been found before the second earthquake event; this may be related to the heavy and cumulative rainfall during this time (red rectangles in Fig. 10a). Also, during heavy and cumulative rainfall, radon value is low; this may be due to the weakening of the capping effect [33, 70] as the water fills the empty pores and reduces the diffusion of radon. Either a

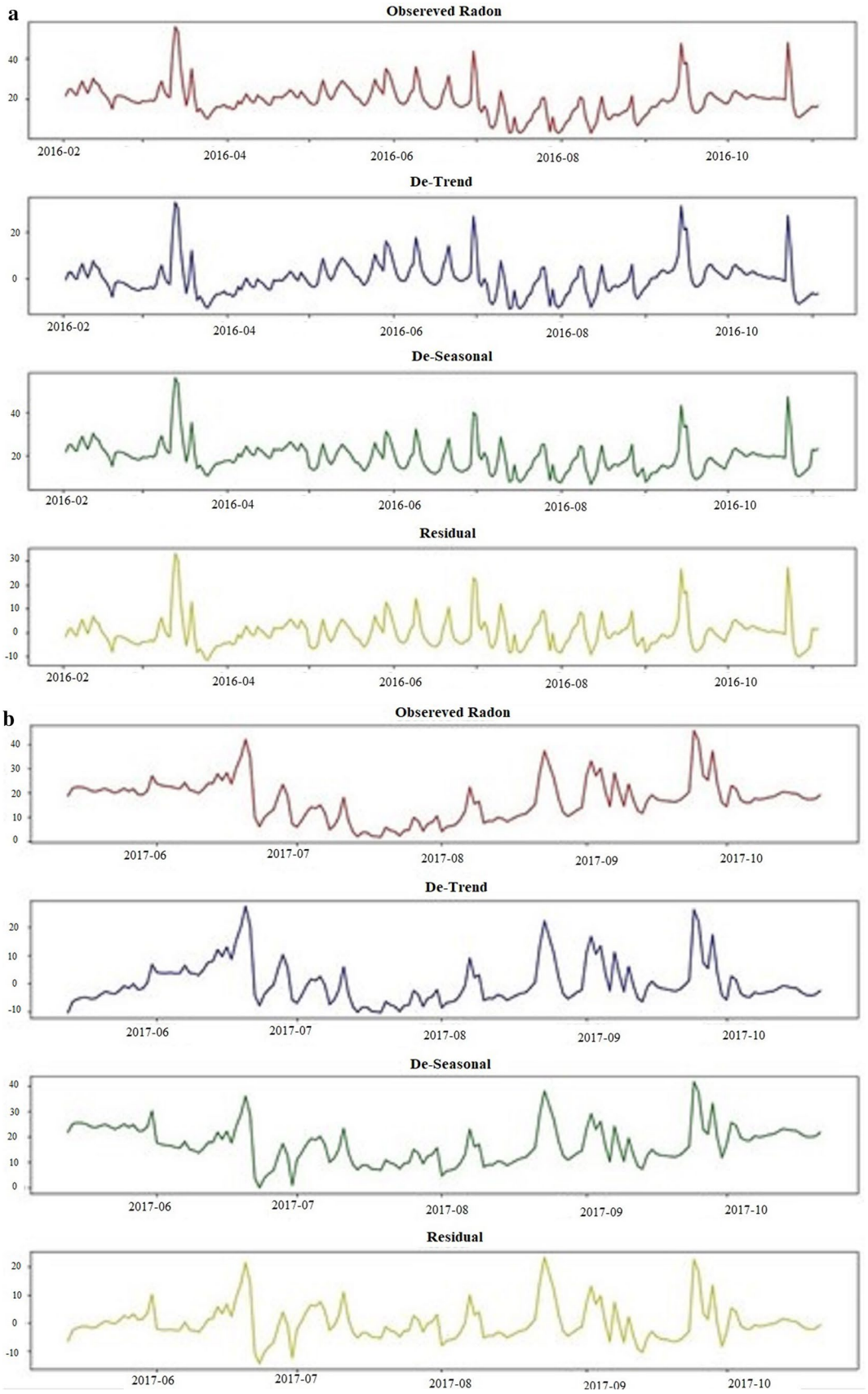
a
Obsereved Radon
40
20
2016-02
2016-04
2016-06
2016-08
2016-10
De-Trend
20
0
2016-02
2016-04
2016-06
2016-08
2016-10
De-Seasonal
40
20
2016-02
2016-04
2016-06
2016-08
2016-10
Residual
30
20
10
0
-10
2016-02
2016-04
2016-06
2016-08
2016-10
b
Obsereved Radon
40
30
20
10
0
2017-06
2017-07
2017-08
2017-09
2017-10
De-Trend
20
10
0
-10
2017-06
2017-07
2017-08
2017-09
2017-10
De-Seasonal
40
30
20
10
0
2017-06
2017-07
2017-08
2017-09
2017-10
Residual
20
10
0
-10
2017-06
2017-07
2017-08
2017-09
2017-10

◂**Fig. 9** Decomposition of the radon time series (from the top first panel is observed radon, the second panel is De-trend, the third panel is De-seasonal, and the fourth panel is residual) using polynomial fitting method **a** for the 2016 and **b** for the year 2017

decrease in the capping effect emerges due to the evaporation of moisture from the topsoil cover or by hydrological factors that make easier the expulsion (squeezing) of water from the upper layer. The irregular patterns in daily radon and residual radon data have been observed two more times but not followed by any earthquake events (black rectangles in Fig. 10a). One of the reasons for that is the light rainfall during this period (capping effect). This is because as rainfall begins, the soil gets humid and the transfer of radon from soil to atmosphere and vice versa is constrained, leading to radon accumulation beneath the thin cap of humid soil [33, 70].

Also, in 2017, four earthquake events having different magnitude (3.1, 4.1, 3.6, and 3.1), that satisfy our criteria have been reported on June 14, 2017, August 16, 2017, September 24, 2017, and October 02, 2017, respectively (Table 1). For the first event, irregular patterns in daily radon, as well as residual radon data, have been recorded just after the event (purple rectangle in Fig. 10b). Before the second event, irregular patterns in residual radon calculated from Statsmodel have been observed and the radon residual value calculated from the polynomial fitting method is close to average (Avg.) plus two standard deviations (2σ). No irregular patterns in daily radon have been recorded before this event. This may be due to the combined effects of the rainfall as well as earthquakes during this time. For the third event, we observed anomalous patters just after it whereas an anomalous pattern before event four has been reported (purple rectangles in Fig. 10b). The irregular patterns in daily radon, as well as residual radon, have been observed two more times but not followed by any earthquake events (black rectangle in Fig. 10b). The possible reason for this might be the light rainfall during this period (capping effect).

In our study, an increase in radon value has been observed before for most of the earthquakes. There are many studies, which have reported increased or decreased radon value before, during, and after the earthquake. An increase in radon was also monitored in soil gas at the foothills of Maragalla, Islamabad before the earthquakes [71]. However, in a similar study carried out in Amritsar Punjab, India [50] has reported increase as well as a decrease in radon value before, during, and after the earthquake events. The study at the multi-parametric geophysical observatory in Assam Valley of Eastern Himalaya, and at Ghuttu, in Garhwal Himalaya India have reported increase as well as a decrease in radon value before, during, and after the earthquake [72, 73].

In the present study, all the seismic events occurring within a distance of 70 km from the monitoring station correlated with the anomalous radon values, except for one seismic event (Table 1). This monitoring station seems to be sensitive only for earthquakes within a distance of 70 km. However, to test and verify it we need more radon acquisition. MBT and MCT are several hundred kilometers long; therefore, soil–gas monitoring in a single location may not provide reliable results. A network of soil–gas monitoring stations is necessary to build up for obtaining reliable observing results to predict seismicity along a fault of several hundred kilometers long.

Conclusions

In the present study, characteristics of temporal variability of soil–gas radon concentrations at the Dharamshala monitoring station, NW Himalaya India have been examined. Pearson correlation was computed by radon against temperature and pressure, and rainfall which was found to be −0.28, −0.22, and −0.15 for 2016, and −0.23, 0.26, and −0.38 for 2017, respectively. The impact of temperature and pressure on radon is not as substantial as the effect of rainfall in this study. The overall influence of rainfall on radon is found to be a week. But local synchrony influence of rainfall on radon is found to be strongest. Apart from meteorological parameter fluctuations, there are possibly more variables that influence the radon emanation and it's also apparent that such dependence can be sophisticated differing from location to location and leading consequently to location-specific characteristics of the radon. The daily radon concentration has been subjected to a detailed analysis for reliable identification of anomalous values using decomposition of time series. The irregular patterns in daily radon are compared with residual radon data for identifying promising anomalous values. The irregular patterns observed in daily radon and residual radon data are caused not only by seismic activities but also associated with heavy and/or cumulative precipitations. In our study, an increase in radon value has been observed before for most of the earthquakes. All the seismic events occurring within 70 km from the monitoring stations correlated with the anomalous radon values, except one event, it can also be concluded that this monitoring station is sensitive to the earthquake occurring within a distance of 70 km. However, to test and verify it we need to generate more radon data. Also, to predict seismicity along a fault of several 1000 km long, it is necessary to build up a network of soil–gas monitoring stations for improving the resolutions of reliable monitoring results. Our results suggest, on a global outlook, that radon can be a potential seismic signature for seismically active regions. Furthermore, we also need to thoroughly study the effect of metrological parameters on radon emission simultaneously to explore valid anomalous values.

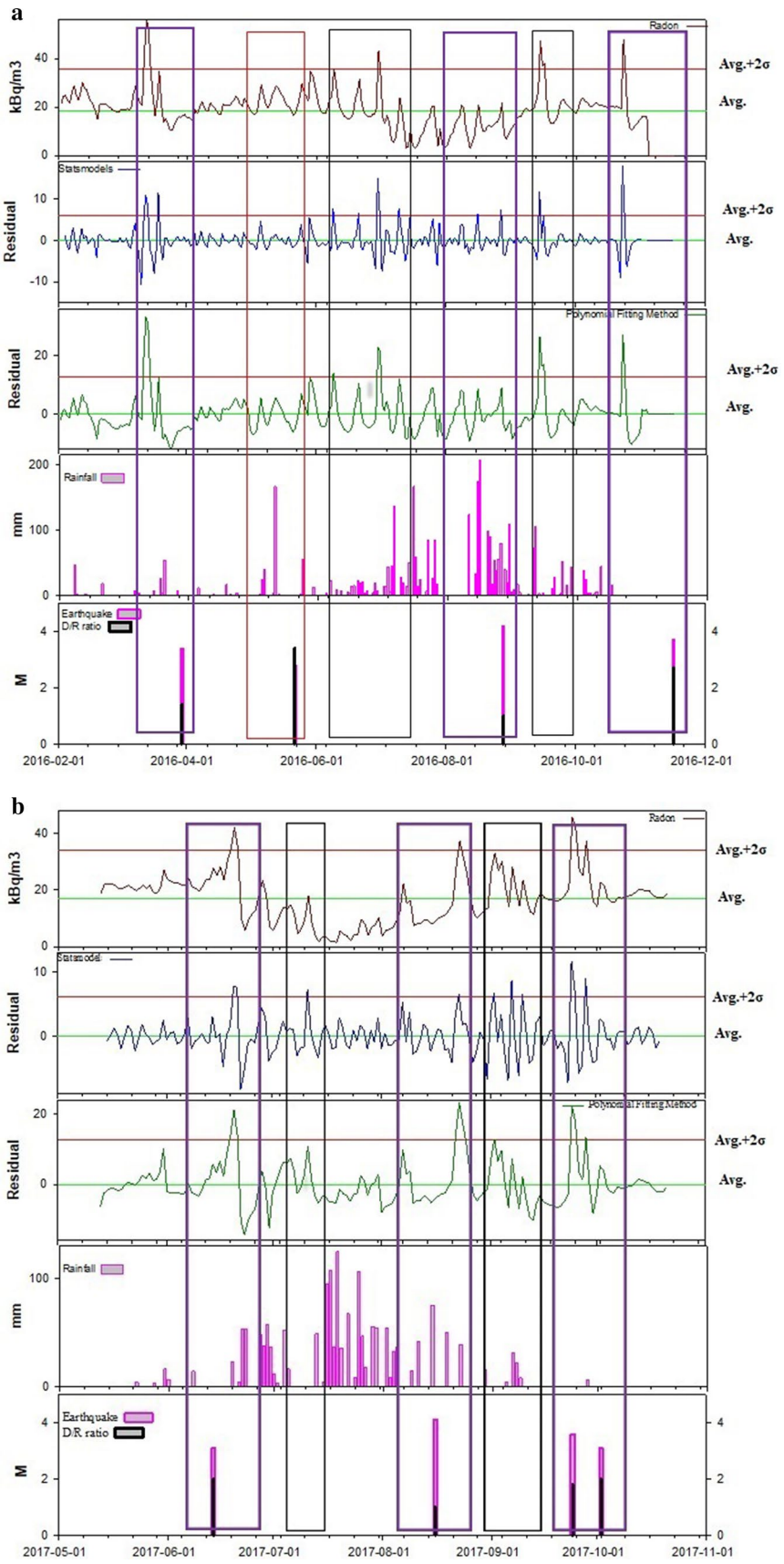

Fig. 10 Correlation of radon anomalies (from the top, the first panel is daily radon, the second panel is residual from Statsmodel, and the third panel is residual from polynomial fitting method) with rainfall (fourth panel) and seismic events (fifth panel) occurred during the study time **a** for the year 2016 and **b** for the year 2017. Purple rectangle shows the earthquake events recorded after and before the irregular patterns in daily radon as well as residual radon data. The red rectangle shows the earthquake events recorded but no irregular patterns in daily radon as well as residual radon data. The black rectangle shows irregular patterns in daily radon as well as residual radon data but no earthquake events

Table 1 Summary of seismic events, rainfall, and radon anomalous values observed during the study period

Date of seismic event (dd/mm/year)	Date of radon anomaly (dd/mm/year)	Latitude (°N)	Longitude (°E)	Depth (km)	Magnitude	Epicentral distance (km)	D/R ratio	Rainfall before or during anomalous value
30/03/2016	13/03/2016	76.1	32.5	10	3.4	39	1.4	No
22/05/2016	No anomaly	76.2	32.7	10	2.9	54	3.4	Yes
No event	30/06/2016							Yes
28/08/2016	16/08/2016 27/08/2016	76.0	32.7	5	4.2	59	1.0	Yes
No event	14/09/2016							Yes
16/11/2016	23/10/2016	75.8	31.4	10	3.7	106	2.7	No
14/062017	20/06/2017	76.5	32.9	5	3.1	44	2.0	No
16/08/2017	07/08/2017	76.3	32.7	10	4.1	45	1.0	Yes
No event	22/08/2017– 10/09/2017							Yes
24/09/2017	24/09/2017	76.2	32.8	5	3.6	65	1.8	No
02/10/2017	28/09/2017	76.7	32.5	5	3.1	44	2.0	No

Acknowledgements Authors thankfully acknowledge the financial support from the Himachal Pradesh Council for Science Technology and Environment (HIMCOSTE) for undertaking this joint study of HIMCOSTE and the Government Post Graduate College Dharamshala as part of the R&D program of HIMCOSTE. The India Meteorological Department (IMD), the Government of India for providing necessary meteorological and seismological data used in this study are also acknowledged.

References

1. OECD (2008) Costs of inaction of environmental policy challenges report ENV/EPOC (2007)17/REV2
2. Sharma S, Dasgupta A, Kumar A, Bharanidharan B, Mittal H, Sachdeva R (2014) Earthquake activity in Kishtwar–Dharamshala region of North-West Himalaya. Int J Adv Res 2(8):463–470
3. Vishwa BSC, Brar KK (2010) Seismicity and vulnerability in Himalayas: the case of Himachal Pradesh, India. Geomat Nat Hazards Risk 1(1):69–84
4. King CY, Igarashi G (2002) Earthquake-related hydrologic and geochemical changes. Int Handb Earthq Eng Seismol 81A:637–645
5. Yang TF, Fu CC, Walia V, Chen CH, Chyi LL, Liu TK, Song SR, Lee M, Lin CW, Lin CC (2006) Seismogeochemical variations in SW Taiwan: multi-parameter automatic gas monitoring results. Pure Appl Geophys 163:693–709
6. Cicerone RD, Ebel JE, Britton J (2009) A systematic compilation of earthquake precursors. Tectonophysics 476:371–396
7. Matsumoto N, Koizumi N (2011) Recent hydrological and geochemical research for earthquake prediction in Japan. Nat Hazards 69:1247–1260
8. Martinelli G (2015) Hydrogeological and geochemical precursors of earthquakes: an assessment for possible applications. Boll Geofis Teor Appl 56(2):83–94
9. King CY, Zhang W, Zhang Z (2006) Earthquake-induced groundwater and gas changes. Pure Appl Geophys 163::633–645
10. Koike K, Yoshinaga T, Ueyama T, Assue H (2014) Increased radon-222 in soil gas because of cumulative seismicity at active faults. Earth Planets Space 66:57
11. Fu CC, Yang TF, Chen CH, Lee LC, Wu YM, Liu TK, Walia V, Kumar A, Lai TH (2017a) Spatial and temporal anomalies of soil–gas in northern Taiwan and its tectonic and seismic implications. J Asian Earth Sci 149:64–77
12. Walia V, Yang TF, Lin SJ, Hong WL, Fu CC, Wen KL, Chen CH (2009a) Geochemical variation of soil–gas composition for fault and earthquake precursory studies along Hsincheng fault in NW Taiwan. Appl Radiat Isot 67:1855–1863
13. Chen Z, Li Y, Liu Z, Wang J, Zhou X, Du J (2018) Radon emission from soil gases in the active fault zones in the capital of China and its environmental effects. Sci Rep 8:16772
14. Walia V, Yang TF, Kumar A, Fu CC, Chiu JM, Chang HH, Wen KL, Chen CH (2012) Temporal variation of soil–gas compositions for earthquake surveillance in Taiwan. Radiat Meas 50:154–159
15. Walia V, Virk HS, Yang TF, Mahajan S, Walia M, Bajwa BS (2005) Earthquake prediction studies using radon as a precursor in N–W Himalayas, India: a case study. Terr Atmos Oceanic Sci 16:775–804
16. Walia V, Yang TF, Lin SJ, Hong WL, Fu CC, Wen KL, Chen CH (2009b) Continuous temporal soil–gas composition variations for earthquake precursory studies along Hsincheng and Hsinhua faults in Taiwan. Radiat Meas 44:934–939
17. Nicoli L, Massimiani G, Segantin S, Zucchetti M (2019) Detection of radon emissions during 2016/2017 earthquakes in Abruzzo (Italy). Fresenius Environ Bull 28(2):672–680
18. Fu CC, Walia V, Yang TF, Lee LC, Liu TK, Chen CH, Kumar A, Lai TH, Wen KL (2017b) Preseismic anomalies in soil–gas radon associated with 2016 M6.6 Meinong earthquake, Southern Taiwan. Terr Atmos Ocean Sci 28(5):787–798
19. Fu CC, Yang TF, Tsai MC, Lee LC, Liu TK, Walia V, Chen CH, Chang WY, Kumar A, Lai TH (2017c) Exploring the relationship between soil degassing and seismic activity by continuous radon monitoring in the longitudinal valley of eastern Taiwan. Chem Geol 469:163–175
20. Megonigal JP, Brewer PE, Knee K (2020) Radon as a natural tracer of gas transport through trees. New Phytol 225(4):1470–1475
21. Papastefanou C (2007) Measuring radon in soil–gas and groundwater: a review. Ann Geophys 50:569–574
22. Zhang W, Zhang Y, Sun Q (2019) Analyses of influencing factors for radon emanation and exhalation in soil. Water Air Soil Pollut 230:16

23. Kovács T, Shahrokhi A, Sas Z, Vigh T, Somlai J (2017) Radon exhalation study of manganese clay residue and usability in brick production. J Environ Radioact 168:15–20
24. Yang J, Busen H, Scherb H, Hürkamp K, Guo Q, Tschiersch J (2019) Modeling of radon exhalation from soil influenced by environmental parameters. Sci Total Environ 656:1304–1311
25. Sas Z, Szántó J, Kovács J, Somlai J, Kovács T (2015) Influencing effect of heat-treatment on radon emanation and exhalation characteristic of red mud. J Environ Radioact 148:27–32
26. Martino SD, Sabbarese C, Monetti G (1998) Radon emanation and exhalation rates from soils measured with an electrostatic collector. Appl Radiat Isot 49(4):407–413
27. Walia V, Yang TF, Lin SJ, Kumar A, Fu CC, Chiu JM, Chang HH, Wen KL, Cheng CH (2013) Temporal variation of soil–gas compositions for earthquake surveillance in Taiwan. Radiat Meas 50:154–169
28. Fu CC, Wang PK, Lee LC, Lin CH, Chang WY, Giuliani G, Ouzounov D (2015) Temporal variation of gamma rays as a possible precursor of earthquake in the longitudinal valley of Eastern Taiwan. J Asian Earth Sci 114(2):362–372
29. Fu CC, Lee LC, Yang TF, Lin CH, Chen CH, Walia V, Liu TK, Ouzounov D, Giuliani G, Lai TH, Wang PK (2019) Gamma ray and radon anomalies in northern Taiwan as a possible pre earthquake indicator around the plate boundary. Geofluids 4734513:14
30. Smetanová I, Holý K, Müllerová M, Anna P (2010) The effect of meteorological parameters on radon concentration in borehole air and water. J Radioanal Nucl Chem 283:101–109
31. Jaishi HP, Singh S, Tiwari RP, Tiwari RC (2014) Correlation of radon anomalies with seismic events along Matfault in Serchhip District, Mizoram, India. Appl Radiat Isot 86:79–84
32. Kumar A, Walia V, Arora BR, Yang TF, Lin SJ, Fu CC, Chen CH, Wen KL (2015) Identifications and removal of diurnal and semi-diurnal variations in radon time-series data of Hsinhua monitoring station in SW Taiwan using singular spectrum analysis. Nat Hazards 79(1):317–330
33. Arora BR, Kumar A, Walia V, Yang TF, Fu CC, Liu TK, Wen KL, Chen CH (2017) Cleaning soil–gas radon at Hsinchu, Taiwan for contamination from meteorological and hydrological parameters: a step forward to identify earthquake precursors. J Asian Earth Sci 149:49–63
34. Choubey VM, Kumar N, Arora BR (2009) Precursory signatures in the radon and geohydrological borehole data for M4.9 Kharsali earthquake of Garhwal Himalaya. Sci Total Environ 407(22):5877–5883
35. Ramola RC, Prasad Y, Prasad G, Kumar S, Choubey VM (2008) Soil–gas radon as seismotectonic indicator in Garhwal Himalaya. Appl Radiat Isot 66(10):1523–1530
36. Siino M, Scudero S, Cannelli V, Piersanti A, D'Alessandro A (2019) Multiple seasonality in soil radon time series. Sci Rep 9:8610
37. Torkar D, Zmazek B, Vaupotic J, Kobal I (2010) Application of artificial neural networks in simulating radon levels in soil gas. Chem Geol 270(1–4):1–8
38. Zmazek B, Todorovski L, Dzeroski S, Vaupotic J, Kobal I (2003) Application of decision trees to the analysis of soil radon data for earthquake prediction. Appl Radiat Isot 58(6):697–706
39. Srikantia SV, Bhargava ON (1998) Geology of Himachal Pradesh. Geological Society of India, Bangalore, 408 pp
40. Kumar S, Mahajan AK (2001) Seismotectonics of the Kangra region, northwest Himalaya. Tectonophysics 331(4):359–337
41. Thakur VC, Jayangondaperumal R, Joevivek V (2018) Seismotectonics of central and NW Himalaya: plate boundary–wedge thrust earthquakes in thin- and thick-skinned tectonic framework. Geol Soc Lond Spec Publ 481:41–63
42. Central Ground Water Board, Division NH, Dharamshala (2013) Groundwater information booklet, District Kangra, Himacahal Pradesh, India. Technical Series E, pp 1–16
43. Dhar S, Randhawa S, Kishore N, Sood RK (2006) Lineament control and seismo-tectonic activity of the areas around Dharamsala, Himalayan Frontal. Zone, Himachal Pradesh, India. Himalayas (Geological Aspects). In: Sakalni PS (ed) vol 4. Satish Serial Publishing House, Delhi, pp 73–78
44. Kumar A, Singh S, Mahajan S, Bajwa BS, Kalia R, Dhar S (2009) Earthquake precursory studies in Kangra valley of north-west Himalayas, India, with special emphasis on radon emission. Appl Radiat Isot 67:1904–1911
45. Galli G, Cannelli V, Nardi A, Piersanti A (2019) Implementing soil radon detectors for long term continuous monitoring. Appl Radiat Isot 153:108813
46. De Simone G, Lucchetti C, Galli G, Tuccimei P (2016) Correcting for H_2O interference using electrostatic collection-based silicon detectors. J Environ Radioact 162–163:146–153
47. Ratner B (2009) The correlation coefficient: Its values range between + 1/–1, or do they? J Target Meas Anal Mark 17:139–142
48. Guerra M, Lombardi S (2001) Soil–gas method for tracing neotectonic faults in clay basins: the Pisticci field (Southern Italy). Tectonophysics 339:511–522
49. Jaishi H, Singh S, Tiwari R, Tiwari R (2014) Temporal variation of soil radon and thoron concentrations in Mizoram (India), associated with earthquakes. Nat Hazards 72(2): 443–454
50. Kumar A, Walia V, Singh S, Bajwa BS, Mahajan S, Dhar S, Yang T (2012) Earthquake precursory studies at Amritsar Punjab, India using radon measurement techniques. Int J Phys Sci 7:5669–5677
51. Singh S, Sharma DK, Dhar S, Randhawa SS (2006) Geological significance of soil–gas radon: a case study of Nurpur area, district Kangra, Himachal Pradesh, India. Radiat Meas 41(4):482–485
52. Ball TK, Nicholson RA, Peachey D (1983) Effects of meteorological variables on certain soil gases used to detect buried ore deposits. Trans Instit of Min Metall 92(b):183–190
53. Rudakov VP (1985) Nature of the seasonal variations in subsoil radon. Geokhimiya 7:133–135
54. Clement WE, Wilkening MH (1974) Atmospheric pressure effects on 222Rn transport across the earth–air interface. J Geophys Res 79(33):5025–5029
55. Singh MR, Ramola C, Singh NP, Singh S, Virk HS (1988) The influence of meteorological parameters on soil–gas radon. J Assoc Expl Geophys 9:85–90
56. Kulali F, Akkurt I, Ozgur N (2017) The effect of meteorological parameters on radon concentration in soil gas. Acta Physica Pol 132(3-II):999–1001
57. Yakut H, Tabar E, Yildirim E, Zenginerler Z, Ertugral F, Demirci N (2017) Soil–gas radon measurement around fault lines on the western section of the North Anatolian fault zone in Turkey. Radiat Prot Dosim 173(4):405–413
58. Piersanti A, Cannelli V, Galli G (2015) Long term continuous radon monitoring in a seismically active area. Ann Geophys 58(4):S437
59. Kainan SUN, Qiuju GUO, Cheng J (2004) The effect of some soil characteristics on soil radon concentration and radon exhalation from soil surface. J Nucl Sci Technol 41(11):1113–1117
60. Piersanti A, Cannelli V, Galli G (2016) The Pollino 2012 seismic sequence: clues from continuous radon monitoring. Solid Earth 7:1303–1316
61. Inan S, Kop A, Cetin H, Kulak F, Pabuccu Z, Seyis C, Ergintav S, Tan O, Saatcilar R, Bodur MN (2012) Seasonal variations in soil radon emanation: long-term continuous monitoring in light of seismicity. Nat Hazards 62(2):575–591
62. Yasuoka Y, Shinogi M (1997) Anomaly in atmospheric radon concentration: a possible precursor of the 1995 Kobe, Japan, earthquake. Health Phys 72:759–761

63. Dagum EB (2010) Time series modeling and decomposition. Statistica 70(4):434–457
64. Nwogu EC, Iwueze IS, Dozie KCN, Mbachu HI (2019) Choice between mixed and multiplicative models in time series decomposition. Int J Stat Appl Math 9(5):153–159
65. Prema V, Rao KU (2015) Time series decomposition model for accurate wind speed forecast. Renewables 2:18
66. Nduka UC, Iwueze SI, Nwogu EC (2017) Fitting polynomial trend to time series by the method of Buys-Ballot estimators. Commun Stat Theory Methods 46(9):4520–4538
67. Dobrovolsky IP, Zubkov SI, Miachkin VI (1979) Estimation of the size of earthquake preparation zones. Pure Appl Geophys 117:1025–1044
68. Hartmann J, Levy JK (2005) Hydrogeological and gas geochemical earthquake precursors: a review for application. Nat Hazards 34:279–304
69. Yang TF, Walia V, Chyi LL, Fu CC, Chen C-H, Liu TK, Song CS, Lee RY, Lee M (2005) Variations of soil radon and thoron concentrations in a fault zone and prospective earthquakes in SW Taiwan. Radiat Meas 40:496–502
70. Schumann RR, Gundersen LCS (1997) Geologic and climatic controls on the radon emanation coefficient. Environ Int 22(1):439–446
71. Barkat A, Ali A, Rehman K, Awais M, Tariq MA, Ahmed J, Amin MA, Iqbal T (2018) Multi-precursory analysis of Phalla earthquake (July 2015; Mw 5.1) Near Islamabad. Pakistan. Pure Appl Geophys 175:4289–4304
72. Chetia T, Sharma G, Dey C, Raju PLN (2020) Multi-parametric approach for earthquake precursor detection in Assam Valley (Eastern Himalaya, India) using satellite and ground observation data. Geotecton 54:83–96
73. Shukla V, Chauhan V, Kumar N, Hazarika D (2020) Assessment of Rn-222 continuous time series for the identification of anomalous changes during moderate earthquakes of the Garhwal Himalaya. Appl Radiat Isot 166:109327